Hindawi Publishing Corporation
Journal of Nanomaterials
Volume 2011, Article ID 267415, 6 pages
doi:10.1155/2011/267415

Research Article

One-Step Nonaqueous Synthesis of Pure Phase TiO_2 Nanocrystals from $TiCl_4$ in Butanol and Their Photocatalytic Properties

Tieping Cao,[1,2] Yuejun Li,[2] Changhua Wang,[1] Changlu Shao,[1] and Yichun Liu[1]

[1] *Centre for Advanced Optoelectronic Functional Materials Research, Key Laboratory for UV Light-Emitting Materials and Technology of Ministry of Education, Northeast Normal University, Changchun 130024, China*
[2] *Faculty of Chemistry, Baicheng Normal University, Baicheng 137000, China*

Correspondence should be addressed to Changlu Shao, changlushao@yahoo.com.cn

Received 10 July 2010; Revised 17 February 2011; Accepted 17 March 2011

Academic Editor: P. Panine

Pure phase TiO_2 nanomaterials were synthesized by an autoclaving treatment of $TiCl_4$ with butanol as a single alcohol source. It was found that the control of molar ratio of $TiCl_4$ to butanol played an important role in determining the TiO_2 crystal phase and morphology. A high molar ratio of $TiCl_4$ to butanol favored the formation of anatase nanoparticles, whereas rutile nanorods were selectively obtained at a low molar ratio of $TiCl_4$ to butanol. Evaluation of the photocatalytic activity of the synthesized TiO_2 was performed in terms of decomposition of organic dye rhodamine B under ultraviolet irradiation. It turned out that the as-synthesized TiO_2 crystallites possessed higher photocatalytic activities toward bleaching rhodamine B than Degussa P25, benefiting from theirhigh surface area, small crystal size as well as high crystallinity.

1. Introduction

The surface photochemistry as well as physical and chemical stability of the semiconductor, TiO_2, makes it an attractive material for multiple applications such as photocatalysis, photovoltaic cells, photochromics, photonic crystals, smart surface coatings, and sensors. Photocatalytic properties of TiO_2 depend significantly on the availability of active sites, and thus, depend on the percentage of exposed surface, surface area, phase composition, and degree of crystallinity [1–10]. TiO_2 exists as three different crystalline structures: rutile, anatase, and brookite. Rutile is the most thermodynamically stable phase, whereas the latter two are metastable phase. Research so far has been centered on the synthesis of anatase nanoparticles. However, recently the preparation of nanometer-sized rutile has received increasing attention due to its promising potential as a photocatalyst [11–14]. For this, well-crystallized anatase or rutile TiO_2 nanocrystals with small crystallite size and high surface area are highly desirable.

Besides, nonaqueous and surfactant-free sol-gel routes in organic solvents offer the possibility of enabling the synthesis of pure phase TiO_2 with high crystallinity and well-defined and uniform morphologies [15–19]. Therein, the simplest route to TiO_2 nanocrystals involves the reaction of $TiCl_4$ with alcohol and usually takes place at lower temperature. The alcohol not only acts as the oxygen-supplying agent for TiO_2 but also strongly influences particle size, shape, and even composition and crystal structure. The slow reaction rates in combination with the stabilizing effect of the organic species lead to the formation of highly crystalline products that are often characterized by uniform morphologies and crystallite sizes in the range of just a few nanometers. By reacting $TiCl_4$ with various alcohol homologs, different crystal phases (rutile and anatase) and morphologies (nanoparticles, nanorods) have been obtained. However, to the best of our knowledge, to manipulate the crystal phase and morphologies of TiO_2 nanocrystals using a single alcohol source has not previously been documented in the literature yet. Motivated by the above results, in this work, by reacting $TiCl_4$ with a single alcohol, butanol, we further extend nonaqueous surfactant-free route to synthesize pure phase of anatase or rutile nanocrystals. The results disclose that the reaction of $TiCl_4$ with butanol at a fairly low temperature leads to anatase TiO_2 nanocrystals with sizes between 5 and 10 nm. Moreover, the reaction system can be easily manipulated to

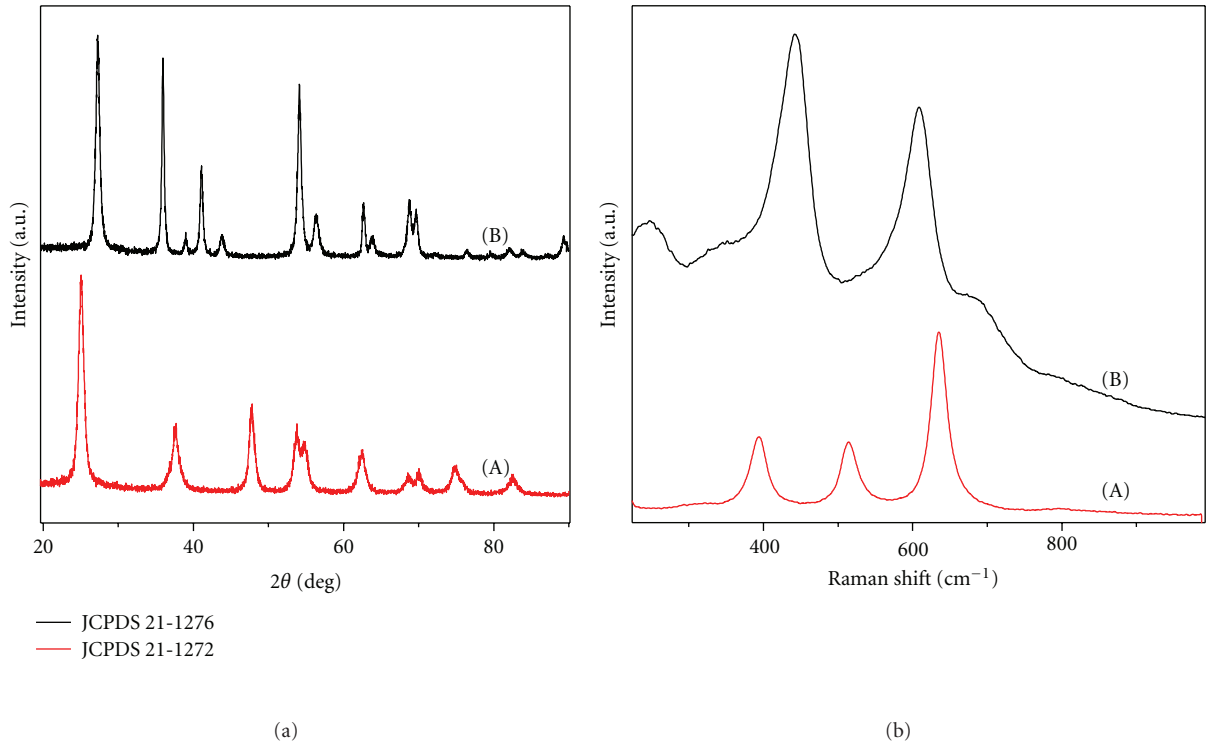

Figure 1: XRD patterns and Raman spectra of TiO_2 samples prepared at high molar ratio of $TiCl_4$ to butanol (A) and low molar ratio of $TiCl_4$ to butanol (B).

produce rutile nanorods with diameters between 10 and 20 nm by simply decreasing the molar ratio of $TiCl_4$ to butanol. Last, the photocatalytic activities of the pure phase TiO_2 nanostructures are evaluated by decomposing the organic dye rhodamine B (RB).

2. Experimental

The procedure for the synthesis of TiO_2 nanomaterials is as follows. A certain molar of $TiCl_4$ (0.005 mol) was quickly dripped into butanol (0.02 or 0.10 mol) under vigorous stirring at room temperature. The pipets and autoclaves were dried in vacuum before use. The obtained solution was transferred to and sealed in teflonlined autoclave (15 mL), and the autoclave was then put in an oven for solvothermal treatment at 150°C for 12 h. The products were collected by filtration, repeatedly washed by ethanol, and dried under vacuum. XRD patterns of the samples were recorded on a Rigaku, D/max-2500 X-ray diffractometer. Raman spectra were recorded on a Jobin-Yvon HR800 instrument with an Ar^+ laser source of 488 nm wavelength in a macroscopic configuration. High-resolution transmission electron microscopy (HRTEM) is performed with a JEM-3010 electron microscope. Nitrogen porosimetry was performed on a Micromeritics ASAP 2010 instrument. Surface areas were calculated using the Brunauer-Emmett-Teller (BET) equation. Pore size distributions were calculated using the Barret-Joyner-Halenda (BJH) model based on nitrogen desorption isotherm.

The photoreactor was designed with an internal light source (50 W high pressure mercury lamp with main emission wavelength 313 nm and an average light intensity of 2.85 mW cm^{-2}) surrounded by a water-cooling quartz jacket to cool the lamp, where a 100 mL aliquot of the RB solution with an initial concentration of 20 mg L^{-1} and TiO_2 solid catalyst (0.1 g) were filled. The solution was stirred in the dark for 30 min to obtain a good dispersion and establish adsorption-desorption equilibrium between the organic molecules and the catalyst surface. Decreases in the concentrations of dyes were analyzed by a Cary 500 UV-VIS-NIR spectrophotometer at $\lambda = 554$ nm. At given intervals of illumination, the samples of the reaction solution were taken out and analyzed.

3. Results and Discussion

XRD and Raman techniques were used to characterize the structure and size of as-obtained nanomaterials. The XRD patterns (Figure 1(a)) clearly demonstrate that the nanomaterials obtained with high molar ratio of $TiCl_4$ to butanol are of anatase phase (JCPDS 21-1272). In contrast, a rutile sample (JCPDS 21-1276) is produced in the synthesis with a low molar ratio of $TiCl_4$ to butanol. The crystallite sizes, using the well-known Scherrer equation based on the half widths of (101) diffraction peak for anatase and (110) diffraction peak for rutile are 8.7 and 15.6 nm for the titania prepared at high and low molar ratio of $TiCl_4$ to butanol, respectively. Moreover, the XRD pure phase anatase and

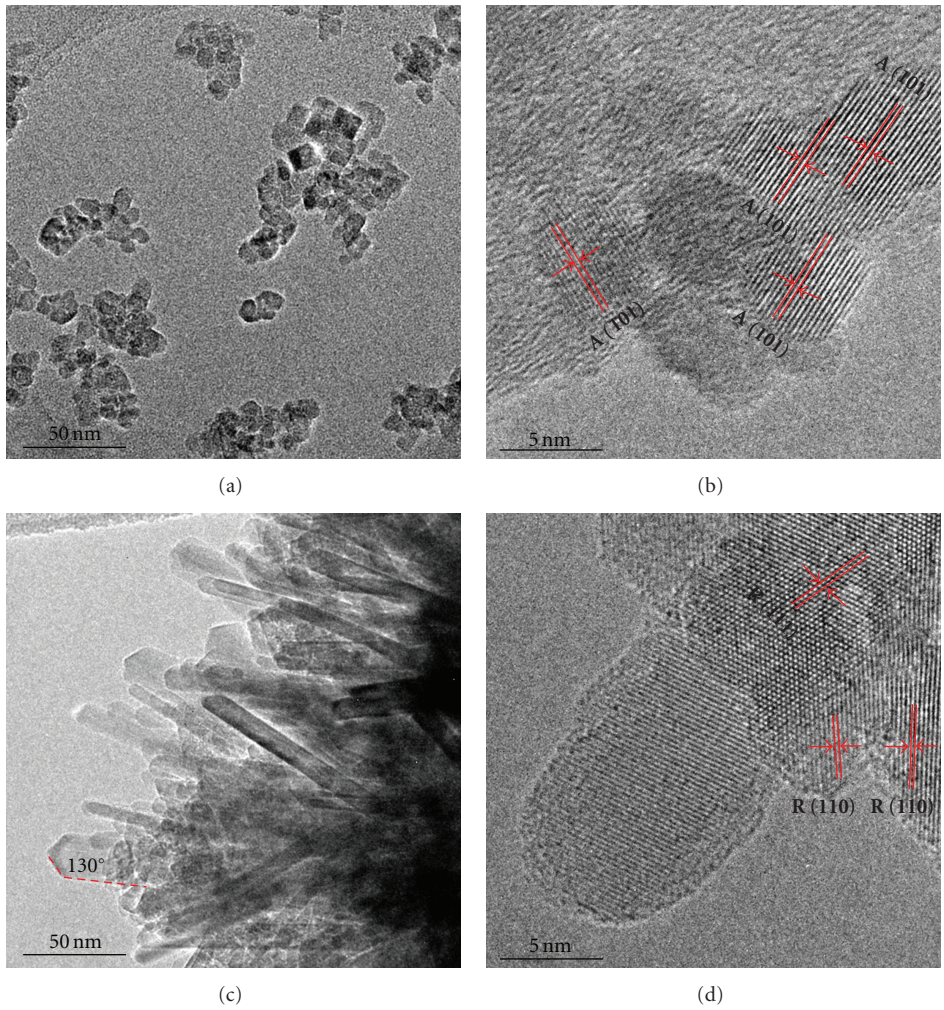

Figure 2: TEM and HRTEM images of anatase nanoparticles (a, b) and rutile nanorods (c, d).

rutile TiO_2 in the Raman spectra further confirms the single phase feature of the TiO_2 products in our present approach. That is, the spectrum of anatase TiO_2, obtained at low molar ratio of $TiCl_4$ to butanol, reveals three Raman bands at 606, 437, and 243 cm^{-1} ranging between 200 and 800 cm^{-1}. The Raman bands at 393, 514, and 614 cm^{-1} are attributed to the anatase sample obtained at high molar ratio of $TiCl_4$ to butanol. No Raman active peaks for any impurities attributed to organic species further indicates that the rutile and anatase phase of TiO_2 thus obtained are of good quality.

The sample powders were further characterized with TEM and HRTEM to gain information on the morphology and size distribution of the crystallites. In the TEM images (Figure 2(a)), the anatase crystallites appeared as uniform irregular particles with sizes close to their XRD crystallite sizes. The diameter of the anatase nanoparticles ranges from 5 to 10 nm. Figure 2(b) shows the HRTEM image of individual particles. The fringes observed are corresponding to the interplanar distances, which agree well with the lattice spacing of the (101) low-index facets of the anatase TiO_2. Moreover, the well-developed lattice fringes clearly indicate the high crystallinity. Figure 2(c) shows the TEM image of rutile crystallites. It can be seen that the crystallites show rod-like feature and the nanorods have a diameter of 10–20 nm. Moreover, most of the nanorods have sharp tips, and the measured angle between the tip edge and main-body side of the nanorod is about 130°, indicating the high crystallinity of rutile nanorods. Since contact angles between (110) and (101), (110) and (111), and (110) and (221) planes are calculated to be 112.5°, 132.3°, and 151.2°, respectively, using the tetragonal rutile unitcell, the angle 130° in this case is attributed to the contact between (110) and (111) planes based on the interplanar angles. More information about the rutile crystals can be derived form the HRTEM image. The lattice spacings being about 0.32 and 0.22 nm between adjacent lattice planes of the TiO_2, nanorods are corresponding to the distance between (110) and (111) crystal planes of the rutile phase, respectively. Therefore, the growth directions of nanorods are concluded to be perpendicular to (110) crystal planes. The preferential growth along this direction is arising from the unique crystal structure of rutile. It is known that rutile has 4_2 screw axes along [001] direction [20]. The screw structure will promote the crystal growth along this direction, leading to a crystal morphology dominated

by the (110) faces, and thereof the size calculated from the broadening of the 110 peak in the XRD pattern corresponds to the diameter of the nanorods. As expected, the results of XRD analysis are consistent with the TEM observation. It is therefore very clear that the change of the molar ratio of $TiCl_4$ to butanol is feasible for control of the crystal phase, and morphology of the TiO_2 materials.

The porous structures of the resulting samples were studied by nitrogen sorption. Figure 3 presents the nitrogen adsorption-desorption isotherms and BJH pore size distribution curves of the samples. The anatase nanoparticles exhibit a type IV adsorption isotherm with an H3 hysteresis loop according to BDDT classification, which is a typical characteristic of mesoporous materials. Herein, formation of such mesoporous structure is attributed to the aggregation of the primary nanoparticles. The surface area and median pore diameters derived from isotherm are 132 $m^2\,g^{-1}$ and 20 nm, respectively. As for the rutile nanorods, the hysteresis loop appears at $0.78 < P/P_0 < 1.0$ in the isotherms, corresponding to the filling of textural macropores produced by rutile nanorods aggregates. The surface area of the as-obtained rutile sample is 83 $m^2\,g^{-1}$.

The data presented above demonstrate that the as-adopted nonaqueous solventhermal process enable highly flexible manipulation of the crystal phase and morphology of TiO_2 nanomaterials by reacting of $TiCl_4$ with single alcohol. More importantly, the synthesis route is one-step, template-free, surfactant-free, as well as performed at low temperature. The reaction can be described as follows [18, 19]:

$$\begin{aligned}
&TiCl_4 + xCH_3CH_2CH_2CH_2OH \\
&\quad \longrightarrow TiCl_{4-x}(CH_3CH_2CH_2CH_2O)x + xHCl \\
&2CH_3CH_2CH_2CH_2OH \\
&\quad \longrightarrow CH_3(CH_2)_3O(CH_2)_3CH_3 + H_2O \\
&TiCl_4 + xH_2O \longrightarrow Ti(OH)_xCl_{4-x} + xHCl \\
&Ti(OH)_xCl_{4-x} \longrightarrow TiO_2 + (4-x)HCl + (x-2)H_2O.
\end{aligned} \tag{1}$$

At the initial stage of mixing, $TiCl_4$ reacts with butanol producing $TiCl_{4-x}(CH_3CH_2CH_2CH_2O)_x$, $CH_3CH_2CH_2CH_2Cl$, as well as HCl. Owing to the steric hindrance of butanol, the reaction is not vigorous and so is the evolution of HCl. Therefore, a certain amount of HCl can be dissolved in butanol through forming oxonium salts between HCl and butanol. Then the dissolved HCl can act as catalyst for the etherification of butanol in the system, and water is produced as a by-product. The hydrolysis of $TiCl_4$ that follows can produce different $Ti(OH)_{4-x}Cl_x$ species because the ligand field strength of OH^- is higher than that of Clions. In the autoclaving stage at elevated temperatures, the polycondensation of $Ti(OH)_{4-x}Cl_x$ species will easily lead to extensive formation of the Ti-O-Ti network and then crystallization. Moreover, $[OC_4H_9^-]$ can serve as a barrier against the hydrolysis of $TiCl_4$. And this slow reaction rate is also the main reason for the growth of TiO_2 nanostructures with good crystallinity.

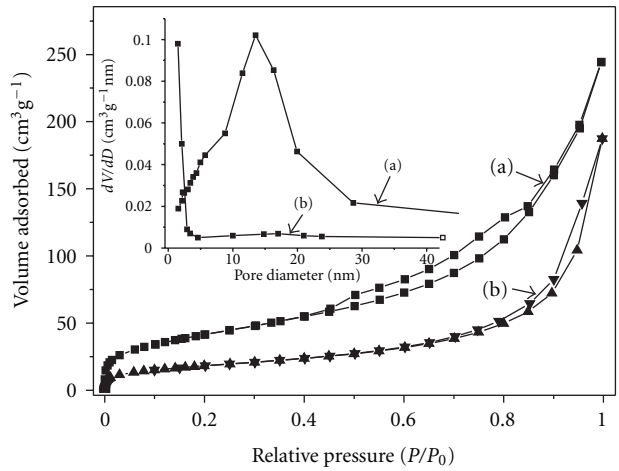

Figure 3: Nitrogen adsorption-desorption isotherm and pore size distribution curve (inset) of anatase nanoparticles (a) and rutile nanorods (b).

The results that pure phase of anatase nanoparticles and rutile nanorods are selectively produced at high and low molar ratio of $TiCl_4$ to butanol, respectively, seems to not agree with the known chemistry in the synthesis of TiO_2 materials in aqueous phase. It has been reported that higher acidity in solution (high molar ratio of $TiCl_4$ to H_2O) could result in the formation of the rutile phase rather than anatase phase. Herein, the difference may be caused by following factors: firstly, when the amount of $TiCl_4$ reactant is fixed, the retention amount of HCl in the reaction system increases as the amount of butanol reactant added increases. The observation that a white acid fog is released from the teflonline tube at high molar ratio of $TiCl_4$ to butanol rather than low molar ratio after opening the autoclave when the autoclave is cooled naturally to room temperature indirectly confirms this. As a result, selective formation of rutile phase is favored in the case of larger amount of HCl retained in the system. Secondly, the steric hindrance of butanol not only serves as a barrier against the hydrolysis of $TiCl_4$ in water but also has the ability to tune the growth behavior of TiO_2 crystals. This has been confirmed by other experimental results. That is, when butanol is replaced by ethanol while other conditions are kept unchanged, only anatase TiO_2 is obtained at both high and low molar ratio of $TiCl_4$ to ethanol. Also, one experiment employing the final solution volume as the condition for rutile synthesis but keeping the molar ratio of $TiCl_4$ to butanol as the condition for anatase synthesis is performed. The result shows that pure anatase phase of TiO_2 is obtained again, suggesting that HCl retained in the system plays important role in the synthesis and the effect of the initial volume of the reactants solution in the autoclave can be neglected. Therefore, the difference of TiO_2 phase and morphology may be attributed to the contribution of the equilibrium concentration of H^+, Cl^-, and steric hindrance effect of butanol. The photocatalytic degradation of RB has been chosen as a model reaction to evaluate the photocatalytic activities of the present samples, and it is compared with that of commercial Degussa P25.

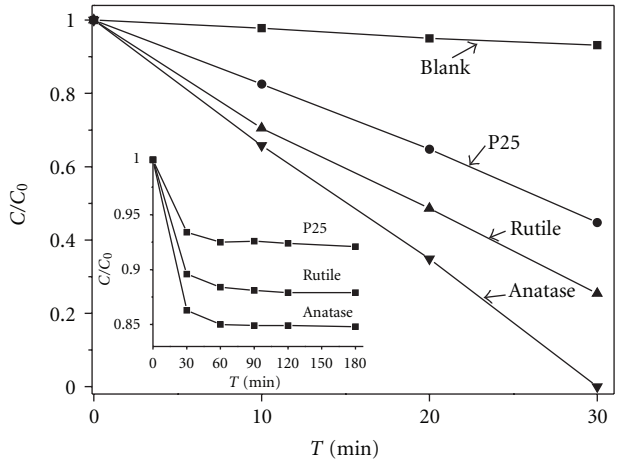

Figure 4: The time course of the photodegradation of RB on UV light-irradiated TiO_2 catalysts; inset shows the adsorption curve in dark over different catalysts.

Figure 4 shows the decolorization curves of RB on different catalysts. The photocatalytic control experiments indicate that there is no appreciable decolorization of RB over TiO_2 either in the absence of UV irradiation or in the absence of the catalyst. However, the absorption peaks corresponding to RB at 554 nm diminishes gradually as the exposure time is extended in the presence of different TiO_2 samples under UV light. The activities of TiO_2 samples are even higher than that of P25. 99, 80, and 60% decolorization of RB are observed after 30 min UV light irradiation for anatase nanoparticles, rutile nanorods, and P25, respectively. Factors including high surface area, small crystal size, and high crystallinity are able to account for the high photocatalytic activities of as-synthesized TiO_2 samples. High surface area can provide more active sites and adsorb more reactive species. Moreover, small crystal size can shorten the route for an electron migrates from the conduction band of TiO_2 to its surface. Meanwhile, the high crystallinity means few defects in photocatalysis. It is well known that lattice defects may act as recombination centers for photoinduced electrons and holes, thus significantly reducing the net photocatalytic activity. Therefore, the as-synthesized highly crystallized anatase nanoparticles and rutile nanorods having diameter of only 5–10 and 10–20 nm, respectively, as well as high surface area of 132 and 83 $m^2\,g^{-1}$, respectively, possess high photocatalytic activity than that of P25 (a mean particle size of 30 nm and specific surface area of 50 $m^2\,g^{-1}$).

4. Conclusion

Summarizing, this work demonstrates that the nonaqueous technique of autoclaving treatment of $TiCl_4$/butanol mixtures can be developed as a new approach for the synthesis of TiO_2 nanocrystallites with controlled crystal size, phase and morphology. The key factor determining the crystal phase and morphology is the molar ratio of $TiCl_4$ to butanol. HCl plays an important role in determining the possible formation mechanism and the crystal structures. The as-adopted approach is one-step, template-free, surfactant-free, as well as performed at low temperature, enlightening a way to synthesize other metal oxides.

Acknowledgments

This work is supported by National High Technology Research and Development Program of China (2006AA03Z311), Cultivation Fund of the Key Scientific and Technical Innovation Project (Grant no. 704017), Ministry of Education of China, National Natural Science Foundation of China (Grant no. 60576040 and 50572014), and Program for New Century Excellent Talents in University (NCET-05-0322).

References

[1] A. Fujishima and K. Honda, "Electrochemical photolysis of water at a semiconductor electrode," *Nature*, vol. 238, no. 5358, pp. 37–38, 1972.

[2] R. Asahi, T. Morikawa, T. Ohwaki, K. Aoki, and Y. Taga, "Visible-light photocatalysis in nitrogen-doped titanium oxides," *Science*, vol. 293, no. 5528, pp. 269–271, 2001.

[3] H. G. Yang, C. H. Sun, S. Z. Qiao et al., "Anatase TiO_2 single crystals with a large percentage of reactive facets," *Nature*, vol. 453, no. 7195, pp. 638–641, 2008.

[4] T. L. Thompson and J. T. Yates, "Surface science studies of the photoactivation of TiO_2—new photochemical processes," *Chemical Reviews*, vol. 106, no. 10, pp. 4428–4453, 2006.

[5] X. Chen and S. S. Mao, "Titanium dioxide nanomaterials: synthesis, properties, modifications and applications," *Chemical Reviews*, vol. 107, no. 7, pp. 2891–2959, 2007.

[6] A. Fujishima, X. Zhang, and D. A. Tryk, "TiO_2 photocatalysis and related surface phenomena," *Surface Science Reports*, vol. 63, no. 12, pp. 515–582, 2008.

[7] J. Zhang, Q. Xu, Z. Feng, M. Li, and C. Li, "Importance of the relationship between surface phases and photocatalytic activity of TiO_2," *Angewandte Chemie International Edition*, vol. 47, no. 9, pp. 1766–1769, 2008.

[8] H. Zhu, X. Gao, Y. Lan, D. Song, Y. Xi, and J. Zhao, "Hydrogen titanate nanofibers covered with anatase nanocrystals: a delicate structure achieved by the wet chemistry reaction of the titanate nanofibers," *Journal of the American Chemical Society*, vol. 126, no. 27, pp. 8380–8381, 2004.

[9] J. C. Yu, L. Zhang, and J. Yu, "Direct sonochemical preparation and characterization of highly active mesoporous TiO_2 with a bicrystalline framework," *Chemistry of Materials*, vol. 14, no. 11, pp. 4647–4653, 2002.

[10] X. Li, X. Quan, and C. Kutal, "Synthesis and photocatalytic properties of quantum confined titanium dioxide nanoparticle," *Scripta Materialia*, vol. 50, no. 4, pp. 499–505, 2004.

[11] A. Testino, I. R. Bellobono, V. Buscaglia et al., "Optimizing the photocatalytic properties of hydrothermal TiO_2 by the control of phase composition and particle morphology. A systematic approach," *Journal of the American Chemical Society*, vol. 129, no. 12, pp. 3564–3575, 2007.

[12] Y. Wang, L. Zhang, K. Deng, X. Chen, and Z. Zou, "Low temperature synthesis and photocatalytic activity of rutile TiO_2 nanorod superstructutes," *Journal of Physical Chemistry C*, vol. 111, no. 6, pp. 2709–2714, 2007.

[13] A. Dessombz, D. Chiche, P. Davidson, P. Panine, C. Chanéac, and J. P. Jolivet, "Design of liquid-crystalline aqueous suspensions of rutile nanorods: evidence of anisotropic photocatalytic properties," *Journal of the American Chemical Society*, vol. 129, no. 18, pp. 5904–5909, 2007.

[14] C. Wang, C. Shao, Y. Liu, and X. Li, "Water—dichloromethane interface controlled synthesis of hierarchical rutile TiO_2 superstructures and their photocatalytic properties," *Inorganic Chemistry*, vol. 48, no. 3, pp. 1105–1113, 2009.

[15] N. Pinna and M. Niederberger, "Surfactant-free nonaqueous synthesis of metal oxide nanostructures," *Angewandte Chemie International Edition*, vol. 47, no. 29, pp. 5292–5304, 2008.

[16] M. Niederberger, "Nonaqueous sol-gel routes to metal oxide nanoparticles," *Accounts of Chemical Research*, vol. 40, no. 9, pp. 793–800, 2007.

[17] I. Djerdj, D. Arčon, Z. Jagličić, and M. Niederberger, "Nonaqueous synthesis of metal oxide nanoparticles: short review and doped titanium dioxide as case study for the preparation of transition metal-doped oxide nanoparticles," *Journal of Solid State Chemistry*, vol. 181, no. 7, pp. 1571–1581, 2008.

[18] C. Wang, Z. X. Deng, and Y. Li, "The synthesis of nanocrystalline anatase and rutile titania in mixed organic media," *Inorganic Chemistry*, vol. 40, no. 20, pp. 5210–5214, 2001.

[19] C. Wang, Z. X. Deng, G. Zhang, S. Fan, and Y. Li, "Synthesis of nanocrystalline TiO_2 in alcohols," *Powder Technology*, vol. 125, no. 1, pp. 39–44, 2002.

[20] K. Kakiuchi, E. Hosono, H. Imai, T. Kimura, and S. Fujihara, "{111}-faceting of low-temperature processed rutile TiO_2 rods," *Journal of Crystal Growth*, vol. 293, no. 2, pp. 541–545, 2006.